Supporting Information

Saur *et al.* 10.1073/pnas.0805234105

SI Methods

MRI Data Acquisition. Structural and functional MRI was performed on a 3T TIM Trio scanner (Siemens) with a standard head coil.

Functional MRI. In cases where the sequence specifications for the repetition experiment differ from the comprehension experiment, values are given in parentheses. A total of 260 (355) scans per session with 36 (30) axial slices covering the whole brain [3 × 3 × 3 (3 × 3 × 3.6) mm^3] was acquired in interleaved order using a gradient echo echo-planar (EPI) T2*-sensitive sequence [TR = 2.19 (1.6) ms, TE = 30, flip angle = 75° (70°), matrix = 64 × 64 $pixel^2$]. During reconstruction, scans were corrected for motion and distortion artifacts based on a reference measurement.

Diffusion Tensor Imaging. We acquired a total of 70 scans with 69 slices using a diffusion-sensitive spin-echo EPI sequence with CSF suppression [61 diffusion-encoding gradient directions (b-factor = 1,000 s/mm), 9 scans without diffusion weighting, voxel size = 2 × 2 × 2 mm^3, matrix size = 104 × 104 $pixel^2$, TR = 11.8 s, TE = 96 ms, TI = 2.3 s]. During reconstruction, scans were corrected for motion and distortion artifacts based on a reference measurement.

MP-RAGE. A high-resolution T1 anatomical scan was obtained (160 slices, voxel size = 1 × 1 × 1 mm^3, TR = 2.2 s, TE = 2.6 ms, FOV = 160 × 240 × 240 mm^3) for spatial processing of the fMRI and DTI data.

fMRI Data Analysis. ***Preprocessing.*** All slices were corrected for different acquisition times of signals by shifting the signal measured in each slice relative to the acquisition of the middle slice. Resulting volumes were spatially normalized to the Montreal Neurological Institute (MNI) reference brain using the normalization parameters estimated during segmentation of the T1 anatomical scan. All normalized images were then smoothed using an isotropic 9 mm Gaussian kernel to account for intersubject differences.

Statistical analysis. At first level, the two conditions (listening to meaningful sentences and pseudo sentences and repeating real words and pseudowords, respectively) were modeled as separate regressors. In the comprehension experiment, onsets of stimuli were convolved with a canonical hemodynamic response function (HRF) as implemented in SPM5. In the repetition experiment, onsets of repetition were defined approximately by the offset of the aurally presented word and convolved with the HRF. In both experiments, voxel-wise regression coefficients for both conditions were estimated using least squares. Our research questions were addressed in a second level analysis for which the contrast images of the conditions were entered into two separate random effects models. Correction for nonsphericity resulting from unequal variances between subjects and conditions was implemented. With respect to our hypotheses, we computed the differential effects between repetition of pseudo words versus real words (sublexical repetition) and listening to meaningful sentences versus pseudo sentences (comprehension).

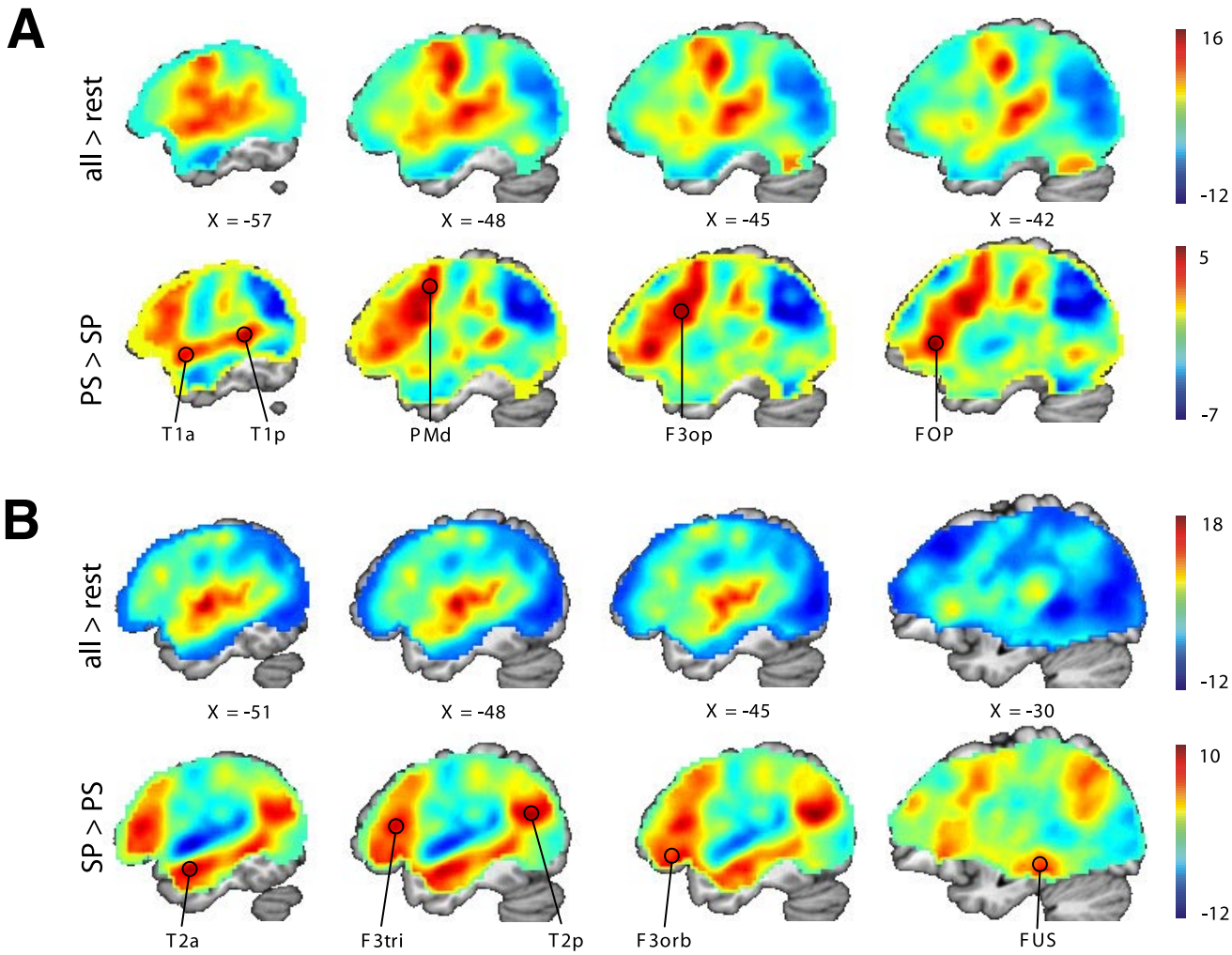

Fig. S1. Auditory repetition and comprehension. Bold activation changes in the repetition (*A*) and comprehension (*B*) experiment displayed as unthresholded *t*-maps. In the upper row, main effects (both experimental conditions vs. rest), in the lower row, differential effects (PS > SP, repetition of pseudowords vs. real words; SP > PS, listening to meaningful sentences vs. pseudo sentences) are displayed. Note the dorsoventral gradient in the temporal lobe in both experiments with inverse activation for speech and pseudo speech stimuli in the superior and middle temporal gyrus.

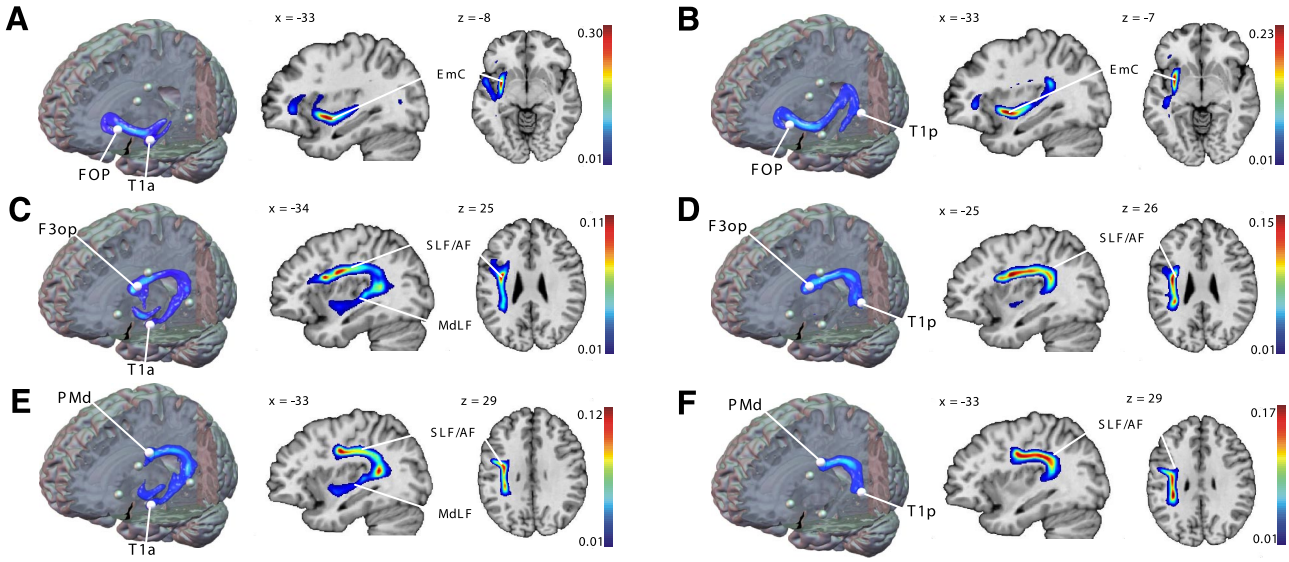

Fig. S2. Temporofrontal fiber pathways subserving repetition. Pairwise region-to-region fiber pathways linking temporal and frontal seed regions defined in the repetition experiment. Three-dimensional tractography renderings are displayed to illustrate the course of each fiber tract. White spheres indicate the seed regions of interest; other seed regions are displayed in semitransparent. Sagittal and axial sections of the group mean maps (no. = 33) are displayed at the peak coordinates of each connection. Maximum PIBI (probability index forming part of the bundle of interest) values are given at the top of the color bar of each connection. Abbreviations of seed regions are as indicated in Fig. 1 and Table 1. EmC, extreme capsule; AF, arcuate fascicle; SLF, superior longitudinal fascicle; MdLF, middle longitudinal fascicle.

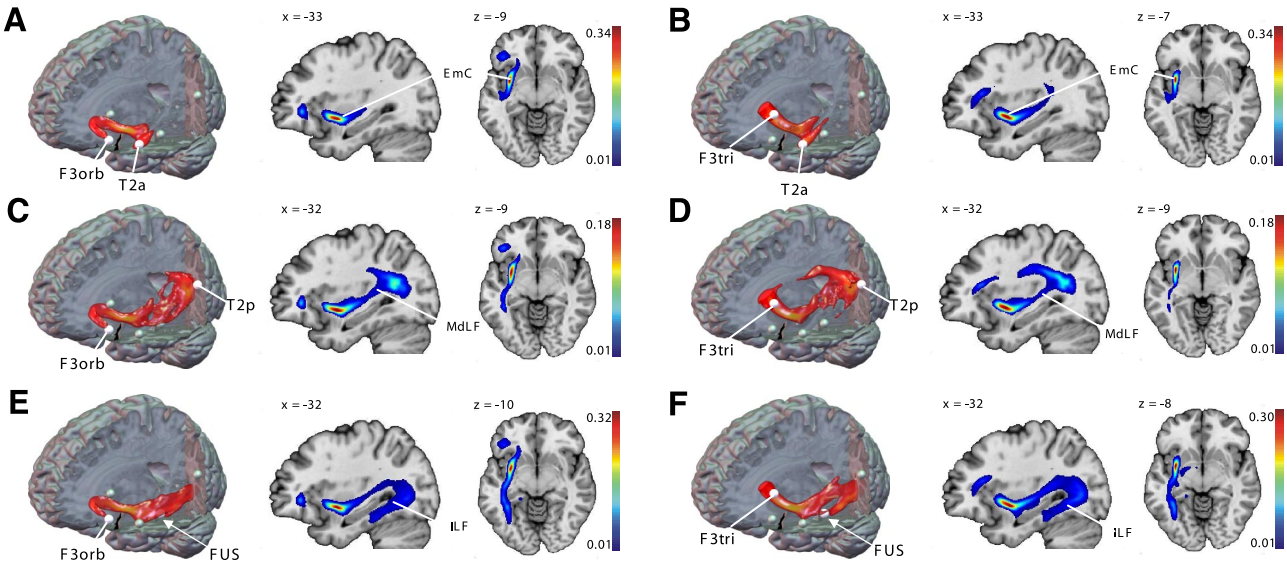

Fig. S3. Temporofrontal fiber pathways subserving comprehension. Pairwise region-to-region fiber pathways linking temporal and frontal seed regions defined in the comprehension experiment. Three-dimensional tractography renderings are displayed to illustrate the course of each fiber tract. White spheres indicate the seed regions of interest; other seed regions are displayed in semitransparent. Sagttal and axial sections of the group mean maps (no. = 33) are displayed at the peak coordinates of each connection. Maximum PIBI (probability index forming part of the bundle of interest) values are given at the top of the color bar of each connection. Abbreviations of seed regions are as indicated in Fig. 1 and Table 2. EmC, extreme capsule; MdLF, middle longitudinal fascicle; ILF, inferior longitudinal fascicle.

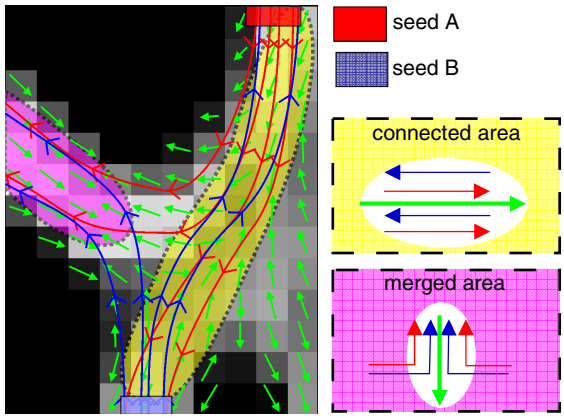

Fig. S4. Connected and merged fibers. Trajectories starting from seed region A (red arrow lines) and B (blue arrow lines) may either face in opposing directions (connecting fibers in the yellow area) or merge and face in the same direction (merging fibers in the magenta area). Within the pathway of interest connecting A and B, the proportion of connecting fibers exceeds the proportion of merging fibers. By calculating the scalar product of the eigenvector (green arrows) and each propagated trajectory, the main traversing direction is determined in each voxel. During multiplication, this directional information is used to suppress merging and preserve connecting fibers. Modified from Kreher *et al.* (10).

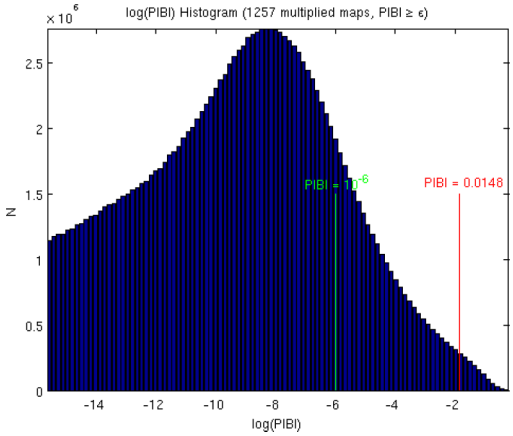

Fig. S5. Distribution of the PIBI (probability index forming part of the bundle of interest) values as extracted from 1,257 preprocessed combined maps. These maps were collected from different experiments, subjects, and connections. The green line at PIBI $= 10^{-6}$ indicates the change of slope which was assumed to indicate the presence of a separate feature in the PIBI distribution, which we attribute to the fiber tracts. Red line indicates the border to the top 5% within this feature.